**POAC'11**
Montréal, Canada

Proceedings of the 21st International Conference on
**Port and Ocean Engineering under Arctic Conditions**
**July 10-14, 2011**
**Montréal, Canada**

POAC11-186

# OIL ENTRAINMENT AND MIGRATION IN LABORATORY-GROWN SALTWATER ICE

Jonas Karlsson [1,2], Chris Petrich [2], Hajo Eicken [2]

[1]University of Copenhagen, Copenhagen, Denmark

[2] Geophysical Institute, University of Alaska Fairbanks, Fairbanks, Alaska, USA

## ABSTRACT

With increased interest in economic development of Arctic resources and waterways, understanding the fate of oil spills in the presence of sea ice becomes crucial for successful spill response and remediation efforts. We performed a series of laboratory experiments to analyze the entrainment and upward migration of oil (Alaska North Slope Crude and synthetic oil) through sea ice as a critical process constraining the timing and strategy of response to oil spills in ice. It was found that oil is entrained into the pore network of growing sea ice and confined to the region near the growing interface where the porosity is above 8 to 15%. This assessment of a minimum entrainment and migration porosity provides a bound on the movement of oil through the microscopic pore network of sea ice. The volume of ice that oil can permeate this way depends on the porosity profile of the ice, which is a function of the temperature profile and bulk salinity profile. Based on these laboratory measurements and consistent observations from past experiments, we hypothesize that stratified oil entrainment takes place if the porosity exceeds a threshold. In addition, oil is able to entrain narrow channels (<2 mm diameter) near the ice–water interface. While the contribution of channel entrainment to the total oil content of the ice is very small, oil in channels appears to be important during the melt season.

## INTRODUCTION

While considerable advances have been made in the understanding of the fate of oil spills in ice-covered waters, numerous aspects have not been quantified to-date (Fingas and Hollebone, 2003). In this study we present new experimental results on the entrainment and movement of oil through laboratory-grown saltwater ice during growth and melt.

The projected continued decline of the Arctic summer sea-ice cover will not eliminate the hazard that ice presents to Arctic shipping and offshore oil exploration. Ice will remain present throughout winter, with significant interannual variability in difficult-to-predict freeze-up and break-up dates. In addition, natural resource development will likely drive increases in year-round shipping operations (AMSA 2009). Oil spills impact the Arctic marine ecosystem (e.g. Jayko et al., 1990) and are a major concern to Arctic residents. Options for oil spill recovery currently available in the Arctic include mechanical methods, bio-remediation, dispersants and in-situ burning. However, oil-spill response in ice-covered waters is much more challenging than response in temperate waters and currently deemed unreliable and untested (AMSA 2009). Apart

from the remoteness and potential logistics challenges, spilled oil is less accessible in ice-covered waters, with the possibility of surface spills in snow or ice, oil pooling among ice floes or in ship channels or release under the ice from pipelines (AMSA 2009). Previous work has been reviewed by Fingas and Hollebone (2003). This study applies to oil spilled under sea ice.

One of the first studies investigating the fate of oil released under sea ice from winter through spring were the NORCOR experiments in landfast first-year sea ice in the Canadian Arctic (NORCOR, 1975; Martin, 1979). They demonstrated that most of the oil spilled in fall and winter was entrained as lenses under the ice. In spring, as the ice started to warm, oil began to migrate upward as brine channels increased in size. Eventually, oil reached the surface through discrete channels in May. As the ice continued to deteriorate, the oil progressively saturated the interstices within and between ice crystals. Oil continued to flow upward through the ice until surface ablation had fully exposed the level of initial oil-lens entrainment. The average concentration of oil in oil-saturated sea ice was 4.5%, with a maximum of 7% in a 4 cm section.

Laboratory experiments similar to work presented here were performed by Otsuka et al. (2004). They grew ice from saltwater of salinity 30 ppt at air temperatures between -15 and -10 ºC. Iranian Crude Oil was injected into a depression at the ice bottom once ice thickness exceeded 150 mm, and the ambient temperature was raised to -5 ºC. Growth was allowed to continue for several days before the ice was sectioned and analyzed for temperature, salinity, porosity and oil content. Based on the description of observations given by Otsuka et al. (2004), oil most likely permeated the interstices directly above the oil lens and entered brine channels. Channels extended to the surface in some experiments. Porosity is the combined fractional volume of non-ice constituents, i.e. air, brine, and oil. The contribution of air to the porosity was assumed to be negligible.

This study is part of a larger international effort to explore the fate of spilled oil and associated water-soluble compounds to inform Arctic oil spill remediation. We investigate modes of oil entrainment and migration through sea ice and the relationship between oil content and porosity. The work complements past measurements to arrive at quantitative relationships and an improved understanding of microstructural controls on oil distribution in ice. To achieve this goal we carried out experiments that further refine past approaches and obtain more detailed information on linkages between ice microstructure, porosity, and oil entrainment and percolation.

## METHODS

Oil infiltration experiments were performed in three different tank set-ups at two different laboratories over the course of three years. Set-ups and methods were conceptually identical but differed in detail, mostly due to differences in tank dimensions and advances in experimental procedures. We limit ourselves to the description of the procedures that worked best since a comparative analysis of all the work is provided in detail by Karlsson (2009).

Common to all experiments is that care was taken to grow ice downward and from water with small and non-negative heat flux in order to obtain a realistic lamellar ice substructure at the ice–water interface (Petrich and Eicken, 2010). While supercooling would have led to the development of a platelet layer, excessive superheating would have resulted in an artificially thin high-porosity layer at the ice–water interface. Pressure build-up in the water was prevented through mechanisms as simple as maintaining a small hole through the ice, and supercooling was further prevented by carefully heating the bottom of the tank. Prior to quantitative oil experiments

presented here, ice fabric and growth conditions were analyzed from horizontal and vertical thin and thick sections of a series of preliminary experiments.

Ice was grown from Instant Ocean salt solution in experiments of the *Exp*-series, and from filtered seawater from Trondheim Fjorden in *SINTEF* experiments. Ice was grown in one of three different insulated tanks: an insulated PVC barrel (experiments Exp 16 and Exp 17, barrel height: 0.95 m, diameter 0.51 m), a plastic container with removable exterior insulation (experiments Exp 20 and Exp 21, container depth: 0.28 m, surface area 0.42 x 0.26 $cm^2$), and an insulated pleaxan cylinder with side window (experiments SINTEF 1 through 3, cylinder height: 0.70 m, diameter: 0.15 m). The surface of the tank was exposed to the laboratory at a controlled air temperature.

Ice temperature profiles and progress of the experiments were recorded with a thermistor probe frozen into the ice. Due to the limited size of the SINTEF-series ice tank, the thermistor probe was frozen into an otherwise identical, adjacent reference tank.

Oil was released under the ice through a U-shaped pipe that was gravity-fed with oil. The U-shaped pipe was introduced under the ice through an access hole obtained by freezing two layers of lubricated tubes into the ice and removing the inner tube for access. The bottom of the outer tube extended below the ice to avoid seepage of oil to the surface. This system of oil injection ensured that the injection pipe would not freeze, no oil leaked before the injection, and generally allowed us to avoid the introduction of air bubbles under the ice. The oil temperature was close to the freezing point of the water.

In order to prevent excessive drainage of oil and brine from the porous bottom layer of growing ice, samples were left to grow an ice layer beneath the oil lens prior to sampling. In melt experiments Exp 16 and 17, core 1 was extracted before cooling of the ice, while the remaining data are from cores that were cooled before extraction.

### *Sample Analysis*

Horizontal ice sections were weighed and melted in covered containers. The oil mass was measured after carefully draining brine from the mixture, and bulk salinity was determined from the drained brine with a YSI30 salinometer. The error in the measurement of oil mass was determined from reference measurements with known oil content. Oil mass was systematically overestimated by 0.11 g (i.e. approximately 5 % in the measurement) with standard deviation in the error of 0.16 g. This error is most likely due to incomplete drainage of brine and possibly the formation of an emulsion.

The oil concentration was calculated as the mass ratio of oil and oil-infiltrated sea ice. The porosity of the ice is the sum of volume fraction of the oil and brine volume fraction, the latter being calculated from ice bulk salinity and linearly-interpolated ice temperature. Details are given by Karlsson (2009). Data given by Otsuka et al. (2004) were analyzed the same way to obtain ice porosity.

### *Oil*

The viscosities of Synthetic oil (marketed as Dark Thread Cutting oil) and two samples of the same batch of North Slope Crude oil were measured with a Brookfield DV-II+ viscometer, temperature controlled with a Julabo FB50-HL circulator. Measurements were performed at a shear rate of 8.4 $s^{-1}$. The viscometer was open to ambient air without barrier for volatile compounds. Temperature was cycled and measurements are shown in Table 1 and illustrated in Figure 1.

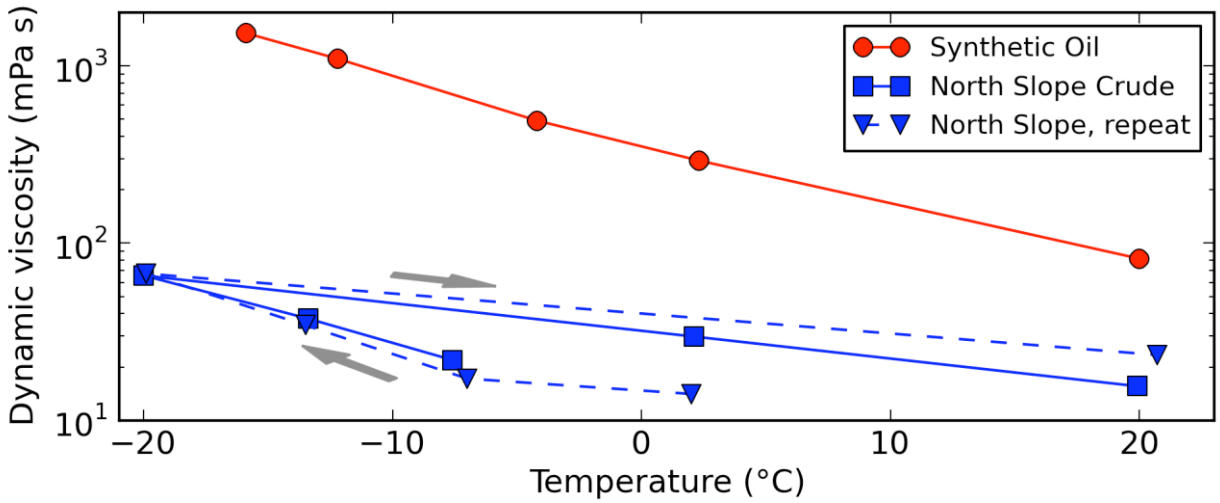


Figure 1. Measured dynamic viscosity of synthetic oil (circles) and North Slope Crude oil. Two samples of North Slope Crude oil were measured (squares, triangles). The arrows indicate the pathway of temperature cycling during the measurements.

Table 1. Viscosity measurements in order of measurement.

| Synthetic Oil | | North Slope Crude | | North Slope Crude, repeat | |
|---|---|---|---|---|---|
| Temperature, °C | Viscosity, mPa s | Temperature, °C | Viscosity, mPa s | Temperature, °C | Viscosity, mPa s |
| 20 | 81.7 | -7.6 | 21.9 | 2 | 14.1 |
| 2.3 | 292 | -13.4 | 37.5 | -7 | 17.2 |
| -4.2 | 490.5 | -20.0 | 65.6 | -13.5 | 34.4 |
| -12.2 | 1094 | 2.1 | 29.7 | -19.9 | 67.2 |
| -15.9 | 1529 | 19.9 | 15.6 | 20.7 | 23.4 |

Table 2. Oil density and viscosity at 5 ºC and shear rate approximately 10 $s^{-1}$. Iranian Light Crude oil was partially evaporated and the shear rate used for Iranian Light Crude is unknown.

| Oil | Viscosity, mPa s | Density, $kg/m^3$ |
|---|---|---|
| Synthetic Oil | 230 | 870 |
| Iranian Light Crude Oil | 45–100 | 857 |
| North Slope Crude Oil | 10 | 834 |
| Kobbe Crude Oil | 11 | 797 |

For reference, extrapolated, approximate viscosity and density data from our measurements for Synthetic oil and North Slope Crude are compared in Table 2 with data for Kobbe Crude oil (Krampa, 2009) and Iranian Light Crude oil. Data given by for Iranian Light Crude oil is valid for partially evaporated oil used in their experiments (Otsuka et al., 2004).

### *Experiments*

In individual experiments ice was grown at an air temperature between -20 and -25 ºC. Once the desired thickness was reached, oil was injected under the ice and the air temperature was adjusted according to Table 3. At the time of release, the oil temperature was between -2 and -1 ºC in all experiments but Exp 20 and 21 where the oil was between 2 and 3 ºC. About 300 ml of oil were released under the ice (Exp 16 and 17: about 500 ml). Oil temperatures in experiments of Otsuka et al. (2004) were considerably higher at 6 to 23 ºC.

Table 3. Key parameters of experiments: oil type, salinity at the start of the experiment, $S_0$, ice thickness at oil release, $H_r$, oil temperature at release, $T_o$, air temperature after oil release, $T_r$.

| Experiment | Oil | $S_0$, ppt | $H_r$, mm | $T_o$, °C | $T_r$, °C |
|---|---|---|---|---|---|
| Exp20 | Synthetic | 28 | 109 | 2.2 | -20 |
| Exp21 | North Slope Crude | 28 | 122 | 2.7 | -20 |
| Exp16 | Synthetic | 32 | 175 | -1.6 | -1 |
| Exp17 | North Slope Crude | 32 | 174 | -1.6 | -1 |
| SINTEF 1 | Kobbe Crude | 34 | 122 | -2 | -25 |
| SINTEF 2 | Kobbe Crude | 23 | 230 | -2 | -25 |
| SINTEF 3 | Kobbe Crude | 56 | 276 | -2 | -25 |
| Otsuka 2, 3, 4, 5 | Iranian Crude | 30 | 150–200 | 12, 6, 19, 23 | -5 |

## RESULTS

During the growth phase of the experiments ice grew at approximately constant growth rate until oil release. Based on control experiments without oil and investigations of excavated samples, the skeletal layer at the ice–water interface was lamellar, as typical of natural columnar ice, without evidence of platelet ice growth (which would have been suggestive of anomalous crystal entrainment from the water column). The bulk salinity profiles of growing ice were C-shaped, as typical for natural sea ice. These observations and individual ice growth and melt conditions are discussed in detail by Karlsson (2009).

At the time of excavation of samples, oil was present both entrained within the ice matrix and encapsulated at the location of the original oil lens. This space is shown in the vertical thick section of Figure 2. Note that the ice is thinnest underneath the lens. The ice layer immediately above the oil lens appears to be almost homogeneously infiltrated with oil; however, the upper boundary of this layer is not sharp. Entrainment further than about 1 cm above the oil lens is restricted to discrete channels. We found from measurements of horizontal sections that the diameter of the channels was below our measurement limit of 2 mm. The oil volume in channel-infiltrated layers was generally too small to measure and is therefore reported as 0.

Figure 3 shows two horizontal thick sections of oil-infiltrated ice after the completion of a melt experiment. Here, oil infiltrated the network of discrete brine channels rather than the entire pore space. The oil concentration increased with porosity, i.e., it is largest near the ice–air interface and the ice bottom. Most notably, there are cm-size patches of oil-free ice in-between oil-infiltrated ice, highlighting the importance of the presence of large channels over average porosity. However, the oil-infiltrated channels were smaller than 2 mm in diameter. In Exp 17, several channels were able to conduct oil to the surface starting 8 days after the ambient temperature was raised to near melting, while no ice reached the surface in Exp 16 by day 15.

Figure 4 shows a scatter plot of oil volume fraction in stratified oil layers above the oil lens and the corresponding porosity for all experiments in Table 4 (Appendix). Although data are scattered, a pattern emerges that is independent of oil type and the particulars of the experiment. Oil was only observed in ice with at least 8% porosity, all ice with porosity above 15% was oil-infiltrated, and the observed oil concentration never exceeded 5%.

## DISCUSSION

Scatter in the results of Figure 4 is to be expected because of incomplete infiltration of the sample volume, either because the sample extended vertically into non-infiltrated ice (Figure 2, 1 cm above the oil lens) or because oil infiltration is patchy laterally (Figure 3). Both effects lead to

underreporting of potential oil content and porosity of locally oil-infiltrated volumes. Hence, the most reliable data for estimating a lower threshold for homogeneous oil infiltration within a layer are those immediately above the oil lens. Therefore, the true lower porosity threshold for homogeneous oil entrainment could be as high as 15%.


Figure 2. Vertical section of (synthetic) oil-infiltrated ice surrounding an overgrown oil lens in an experiment equivalent to Exp 20. Gradation at the sides is in 10 mm.

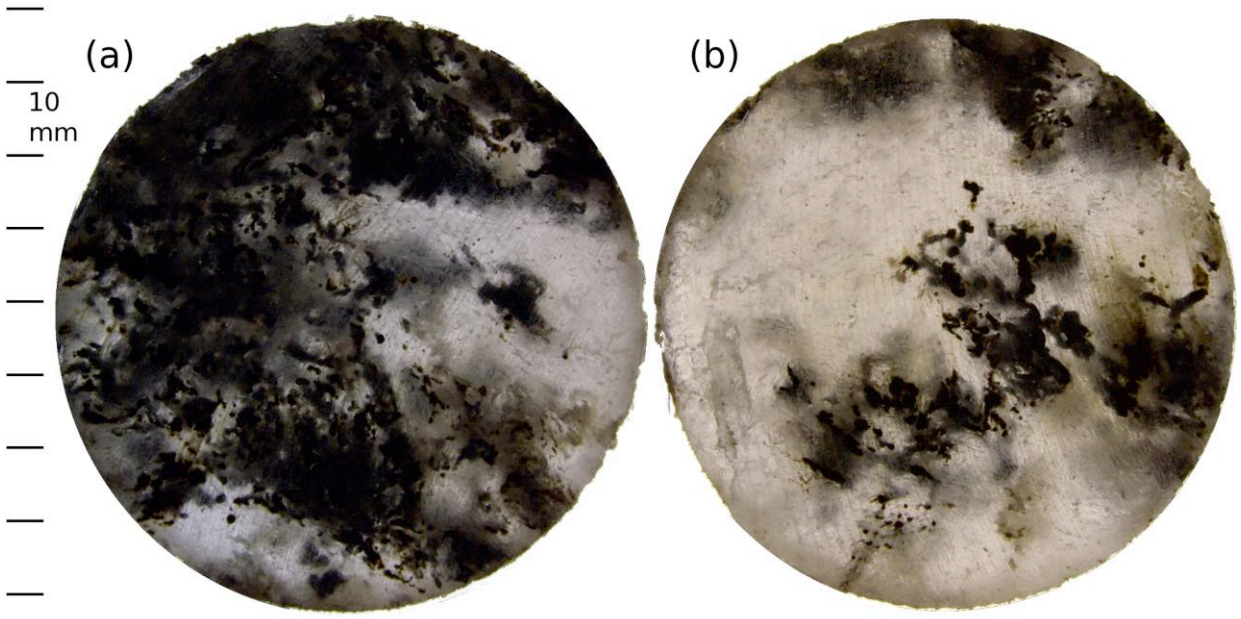


Figure 3. Horizontal thick sections of Exp 17, core 2, at positions (a) -70 mm and (b) -110 mm.

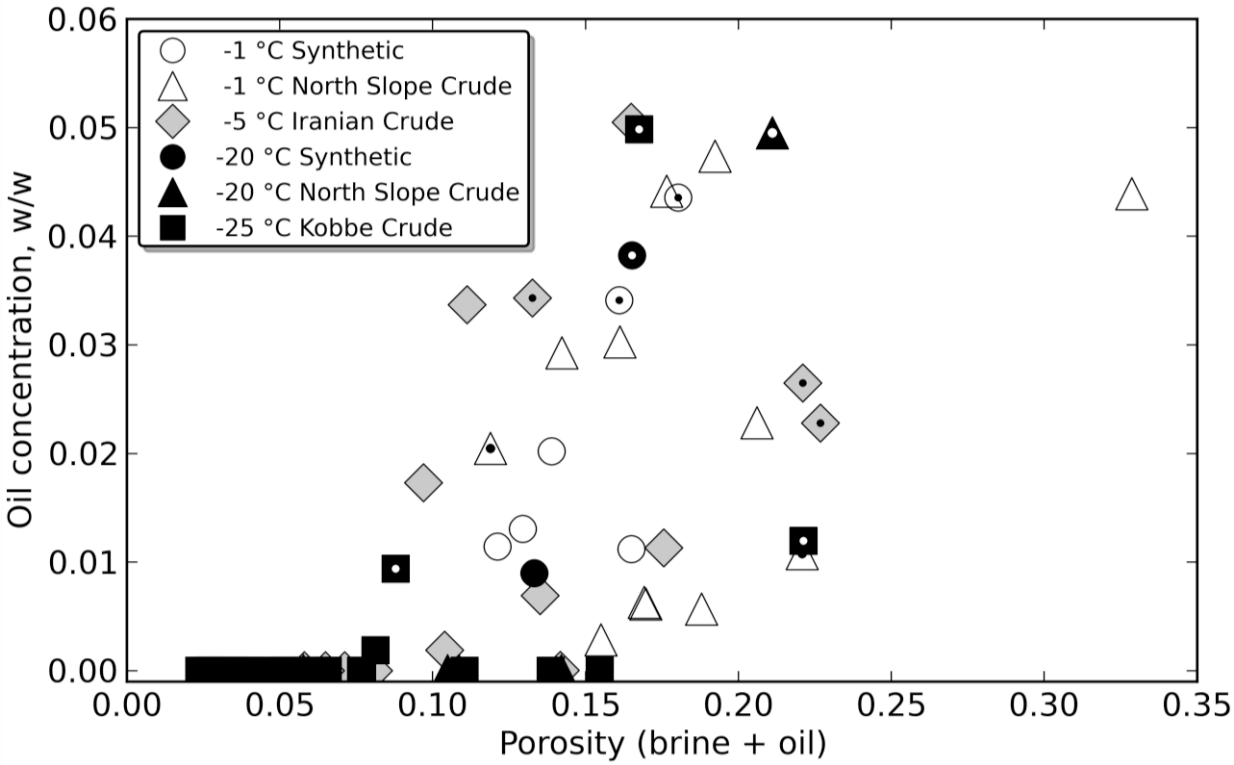


Figure 4. Observed oil concentration (weight of oil divided by weight of sea ice) versus ice porosity (i.e. the sum of brine volume fraction and oil volume fraction) for different oils and boundary conditions. Markers containing a dot indicate data from the bottom-most layer listed in Table 4. Data of Iranian Crude oil are from Otsuka et al. (2004).

Even in cold ice, oil entrained in channels reached higher into the ice than oil entrained in layers (Figure 2). Entrainment of oil in channels is frequently observed in decaying ice. In addition to our observations in Exp 17, NORCOR (1975) reported of preferential percolation of oil through channels during the early stages of melt. While the contribution of channel entrainment may be small compared to the over-all oil content, oil already entrained in channels may enhance oil percolation during the early stages of melt.

Based on the present set of data, we cannot discern a dependence of entrainment on oil temperature at the time of release (Table 3). While concentrations of comparatively warm Iranian Crude Oil define an upper bound, the significance of this notion would have to be examined in dedicated study. However, we cannot exclude that entrainment in individual channels might have been enhanced due to local melting of ice surrounding the channels.

The crude oil viscosity at the end of our laboratory measurements was higher than at the beginning (Figure 1). This could be either because the oil had not reached the desired temperature, or because of outgassing of volatile compounds during the course of the experiments increasing the viscosity. Oil encapsulated in ice will not outgas, suggesting synthetic oil in Exp 16 was of significantly higher viscosity than crude oil in Exp 17. Since Exp 16 and Exp 17 were exposed to the same ambient conditions simultaneously, the absence of oil reaching the ice surface by the end of Exp 16 suggests that oil viscosity may be significant during channel percolation in the melt season.

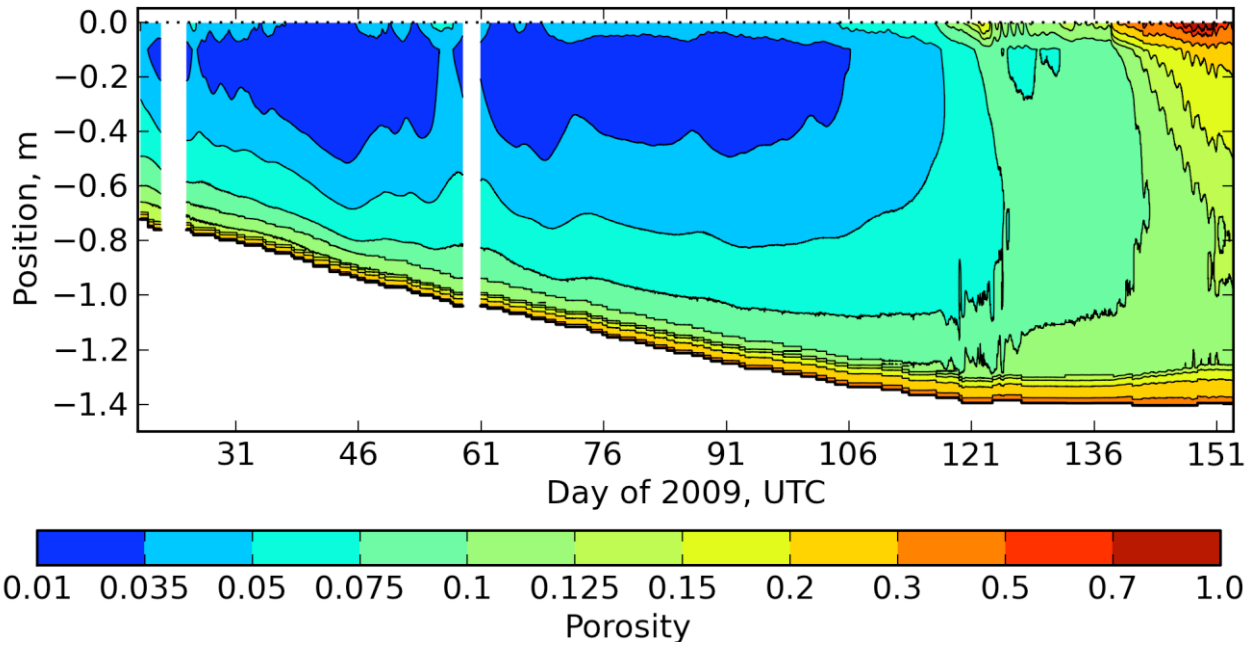


Figure 5. Seasonal profile of porosity (i.e. brine volume fraction) of first-year sea ice at Barrow, Alaska, 2009, inferred from temperature and bulk salinity profile measurements. Note that the porosity scale is non-linear. Porosity was calculated from ice temperature data logged nearly continuously and bulk salinity profiles measured during the season. The non-textbook profile between days 120 and 130 is due to a warm spell. Snow depth during the period shown was between 15 and 25 cm.

## CONCLUSION

Laboratory experiments on entrainment and migration of synthetic and crude oil in artificial sea ice were performed under different boundary conditions. It was found that the ice immediately above the oil lens is oil-saturated, and oil can reach several centimeters into the ice through discrete brine channels, even in cold ice. In spite of notable scatter in the data, the relatively large body of data assembled in this study reveals emerging patterns.

First, oil concentration was never found to exceed 5%. Based on the present experiments, the potential for stratified entrainment in cold sea ice can be estimated by assuming that 5% of the bottom 2 cm are saturated with oil. In this case, the entrainment is about 0.001 $m^3/m^2$, which is significantly less than the typical retention capacity of ice based on under-ice topography, observed to be 0.01 to 0.06 $m^3/m^2$ (Fingas and Hollebone, 2003). Higher volumes for stratified entrainment can be expected for oil spills under warm ice, i.e., in spring and particularly in summer. However, based on limited experimental evidence, oil with significant heat content, such as that emerging from a pipeline, would not get entrained significantly more efficiently in the lower layers of the ice but may possibly be able to penetrate ice upward through brine channels. This would lead to the emergence of oil at the surface earlier in the melt season.

Second, stratified entrainment is limited to ice with porosity above 8 to 15% across a variety of oils and under both growing and melting conditions. Further, we found oil in all samples with porosity larger than 15%. This allows us to estimate that at least some encapsulated oil should be

able to reach the ice surface at the latest when the least porous part of the ice exceeds 15% porosity.

To help illustrate the significance of this porosity range, Figure 5 shows the seasonal variability of porosity determined for landfast sea ice at Barrow, Alaska, 2009. At any time, the porosity was lowest in the ice interior, reaching persistent values above 7.5% not until mid-May. However, even 12.5% porosity throughout the ice was not observed until June. With 15% porosity not observed until about the time of meltpond formation (i.e. first half of June in Barrow), this highlights the importance of investigating the oil migration modes and pathways in more detail to reduce the temporal uncertainty of oil migration to time scales relevant to remediation procedures. In particular, bounds on migration through channels are needed.

The 15%-estimate of an upper limit of porosity necessary for oil migration is consistent with NORCOR (1975) observations, as is the observation that size and density of channels were more relevant to upward oil migration in warm ice than the value of bulk porosity. While some work has been performed quantifying brine channel characteristics (e.g. Wakatsuchi and Saito, 1985), a systematic investigation of the interrelationships between oil content in channels, channel size, air volume fraction and bulk porosity would be would be a promising arena for future work.

## ACKNOWLEDGEMENTS

This work was funded by the Oil Spill Recovery Institute (OSRI), Alaska, USA, and the Coastal Response Research Center (CRRC), New Hampshire, USA. CP was partly supported by an International Polar Year postdoctoral fellowship of the University of Alaska Foundation. Barrow ice temperature and salinity data were acquired under National Science Foundation, USA, award number OPP-0632398 and OPP-0856867. The constructive comments of the reviewer are gratefully acknowledged.

## REFERENCES

AMSA, 2009. Arctic Marine Shipping Assessment 2009 Report. Arctic Council, April 2009.

Fingas and Hollebone, 2003. Review of behavior of oil in freezing environments. Marine Pollution Bulletin, 47, 333–340.

Jayko, K., M. Reed, A. Bowles, 1990, Simulation of interactions between migrating whales and potential oil spills, Environmental Pollution, 63, 97–127.

Karlsson, J., 2009. Oil movement in sea ice. Masters Thesis, University of Copenhagen, Copenhagen, Denmark, 199 pp.

Krampa, F., 2009. FACE Project Viscous Oil Database: v1.0, Technical report, SINTEF.

Martin, S., 1979, A field study of brine drainage and oil entrainment in first-year sea ice, Journal of Glaciology, 22(88), 473–502.

NORCOR Engineering and Research Ltd., 1975. The interaction of crude oil with Actic sea ice. Beaufort Sea Technical Report No. 27. Beaufort Sea Project, Department of the Environment, Victoria, BC, Canada. 201 pp.

Otsuka, N., H. Kondo, H. Saeki, 2004. Experimental study on the characteristics of oil ice sandwich. Proceedings of OCEANS '04 MTS/IEEE—TECHNO-OCEAN '04., vol. 3, 9–12 Nov. 2004, Kobe, Japan. pp. 1470–1475.

Petrich, C. and H. Eicken, 2010. Growth, Structure and Properties of Sea Ice. In Thomas and Dieckmann (eds), Sea Ice, 2nd ed, Wiley–Blackwell, pp. 23–77.

Purves, 1978 The interaction of crude oil and natural gas with laboratory-grown saline ice. Report EPS 4-EC-78-9, Fisheries and Environment Canada, 18 pp.

Wakatsuchi, M. and T. Saito, 1985. On brine drainage channels of young sea ice. Annals of Glaciology, vol.6, 200–202.

## APPENDIX

Table 4. Bulk salinity, temperature, porosity $\varphi$, and oil concentration (w/w) at the time of excavation. Depth is the center of the sample, measured from the ice–air interface. Data of oil-free layers near the upper surface in SINTEF experiments are not shown.

| Exp | Depth, mm | $S$, ppt | $T$, °C | $\varphi$ | Oil conc. |
|---|---|---|---|---|---|
| Exp20 | -86 | 9.7 | -3.8 | 0.13 | 0.010 |
| | -102 | 7.8 | -2.9 | 0.17 | 0.038 |
| Exp21 | -13 | 14.3 | -6.9 | 0.11 | 0 |
| | -34 | 6.3 | -5.5 | 0.06 | 0 |
| | -69 | 7.4 | -3.5 | 0.10 | 0 |
| | -86 | 8 | -2.8 | 0.14 | 0 |
| | -108 | 7.4 | -2.2 | 0.21 | 0.050 |
| Exp16 Core 1 | -30 | 3.5 | -1.1 | 0.17 | 0.011 |
| | -70 | 4.4 | -2.0 | 0.12 | 0.011 |
| | -90 | 4.9 | -2.0 | 0.13 | 0.013 |
| | -110 | 5.1 | -2.1 | 0.14 | 0.020 |
| | -150 | 5.5 | -2.1 | 0.16 | 0.034 |
| Exp16 Core 4 | -110 | 6.0 | -2.1 | 0.18 | 0.043 |
| Exp17 Core 1 | -50 | 7.0 | -1.9 | 0.21 | 0.023 |
| | -70 | 7.2 | -2.0 | 0.19 | 0.006 |
| | -90 | 6.8 | -2.0 | 0.17 | 0.006 |
| | -110 | 6.4 | -2.1 | 0.16 | 0.003 |
| | -130 | 6.8 | -2.1 | 0.17 | 0.006 |
| | -150 | 8.8 | -2.1 | 0.22 | 0.011 |
| Exp17 Core 2 | -30 | 6.6 | -1.1 | 0.33 | 0.044 |
| | -50 | 5.2 | -1.9 | 0.18 | 0.044 |
| | -70 | 6.0 | -2.0 | 0.19 | 0.047 |
| | -90 | 5.6 | -2.0 | 0.16 | 0.030 |
| | -110 | 4.9 | -2.1 | 0.14 | 0.029 |
| | -130 | 4.2 | -2.1 | 0.12 | 0.020 |

| Exp | Depth, mm | $S$, ppt | $T$, °C | $\varphi$ | Oil conc. |
|---|---|---|---|---|---|
| SINTEF 1 | -70 | 7.8 | -14 | 0.03 | 0 |
| | -90 | 8.4 | -12 | 0.04 | 0 |
| | -110 | 10.9 | -10 | 0.06 | 0 |
| | -128 | 12.8 | -8.8 | 0.09 | 0.009 |
| SINTEF 2 | -175 | 5.7 | -8.8 | 0.03 | 0 |
| | -200 | 5.9 | -7.3 | 0.04 | 0 |
| | -225 | 5.9 | -5.6 | 0.05 | 0 |
| | -244 | 6.9 | -4.3 | 0.08 | 0.002 |
| | -256 | 8.4 | -3.3 | 0.17 | 0.050 |
| SINTEF 3 | -180 | 9.6 | -8.3 | 0.06 | 0 |
| | -200 | 10.3 | -7.1 | 0.08 | 0 |
| | -217 | 17.6 | -5.9 | 0.15 | 0 |
| | -231 | 20.0 | -4.8 | 0.22 | 0.012 |
| Otsuka 2 | -25 | 8.3 | -5.9 | 0.07 | 0 |
| | -75 | 5.8 | -5.0 | 0.06 | 0 |
| | -125 | 7.9 | -3.8 | 0.10 | 0.002 |
| | -175 | 12.8 | -3.2 | 0.22 | 0.027 |
| Otsuka 3 | -25 | 7.8 | -4.8 | 0.10 | 0.017 |
| | -75 | 6.5 | -4.0 | 0.11 | 0.034 |
| | -125 | 7.7 | -3.1 | 0.16 | 0.051 |
| Otsuka 4 | -25 | 9.8 | -3.4 | 0.14 | <0.001 |
| | -75 | 7.8 | -3.0 | 0.14 | 0.007 |
| | -125 | 8.3 | -2.5 | 0.18 | 0.011 |
| | -175 | 8.5 | -2.0 | 0.23 | 0.023 |
| Otsuka 5 | -25 | 6.3 | -4.8 | 0.06 | 0 |
| | -75 | 6.3 | -3.8 | 0.08 | 0 |
| | -125 | 5.8 | -2.8 | 0.13 | 0.034 |